

SUPPLEMENTAL MATERIALS

Table S1

NPs	Estimated production volume (t/y)	Application area	Possible exposure routes
Co ₃ O ₄	N/A	<ul style="list-style-type: none"> • Magnetic materials • Heterogeneous catalysts • Electrochromic devices • Solid-state sensors etc. 	Exposure to surface water and sewage by industrial discharge
CuO	N/A	<ul style="list-style-type: none"> • Pigment (ceramics) • Wood preservation • Antimicrobial textile • Antifouling in marine paints • Solar cells • Gas sensor etc. 	Exposure to air, surface water, sewage and soil by industrial discharge and personal use
NiO	N/A	<ul style="list-style-type: none"> • Batteries etc. 	End of life disposal at dump sites, spread to soil
ZnO	600,000	<ul style="list-style-type: none"> • Antibacterial in dentistry • Cosmetics and sunscreens • Display • Solar cells • Photovoltaic cell etc. 	Exposure to air by industrial discharge and personal use, wash-off to surface water and sewage, and soil

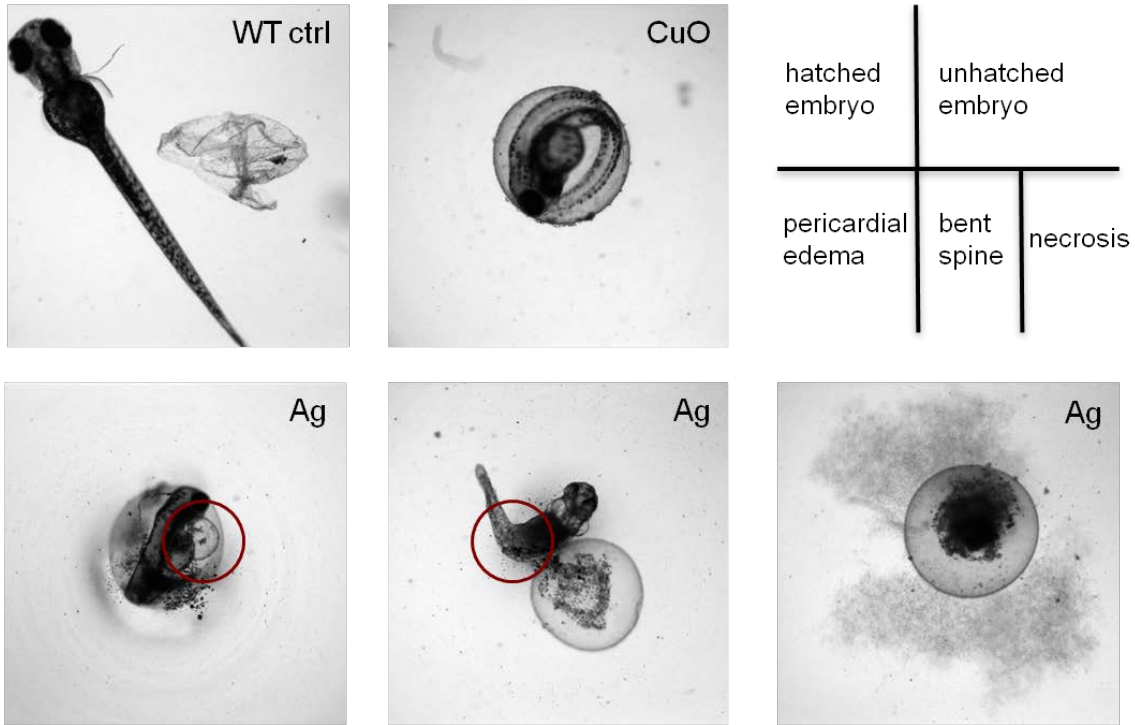


Figure S1. Representative bright-field images of embryos exposed to nanoparticles and collected by automated imaging. Each image was captured automatically through the 2x dry objective of the ImageXpress that autofocuses on every well in the 96-well plate. The high-resolution images allow assessment of hatching, mortality as well as morphological abnormalities such as pericardial edema or bent spine, etc. We included nano-Ag spheres as a positive control to show the morphological abnormalities outlined in the legend. Please notice the difference in appearance of an unhatched live embryo (CuO) as compared to the necrotic embryo seen with Ag.

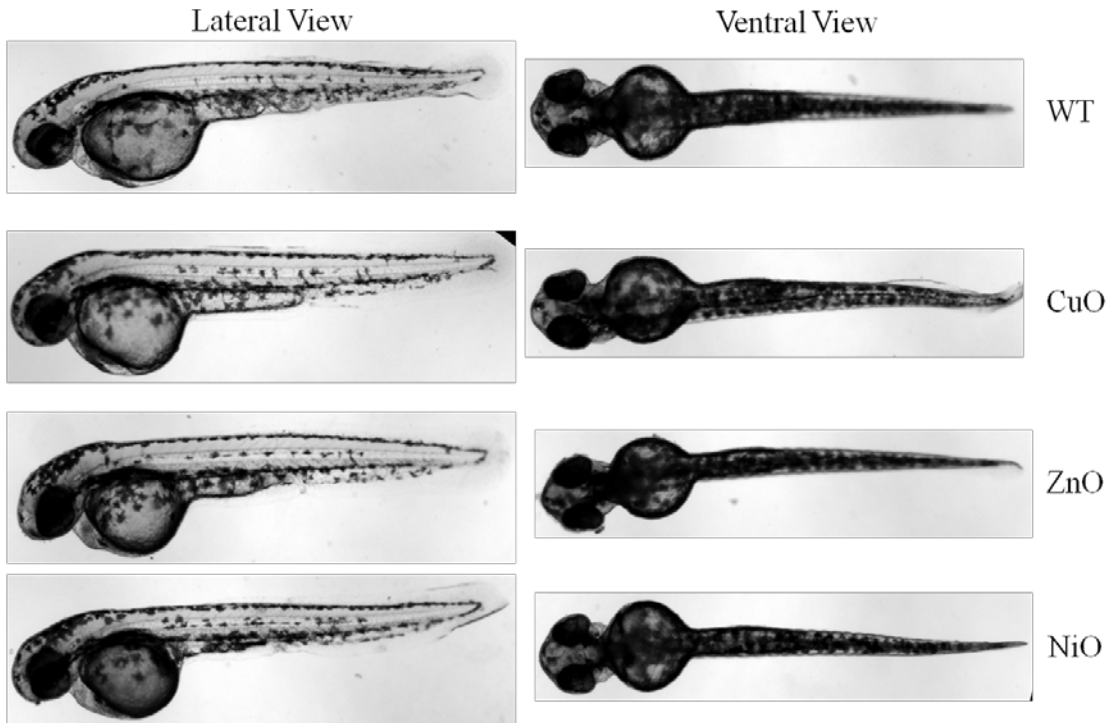


Figure S2. Detailed imaging on wild type controls and embryos exposed to nanoparticles. Wild type controls and embryos exposed to nanoparticles (48 hpf) were collected, anesthetized using 0.017% of tricaine solution for 5 minutes and dechorionated using a fine forceps. The embryos were embedded in low melting agarose gel for positioning. Microscopic imaging was conducted by focusing on lateral and ventral views for comparison (Zeiss Observer D1).

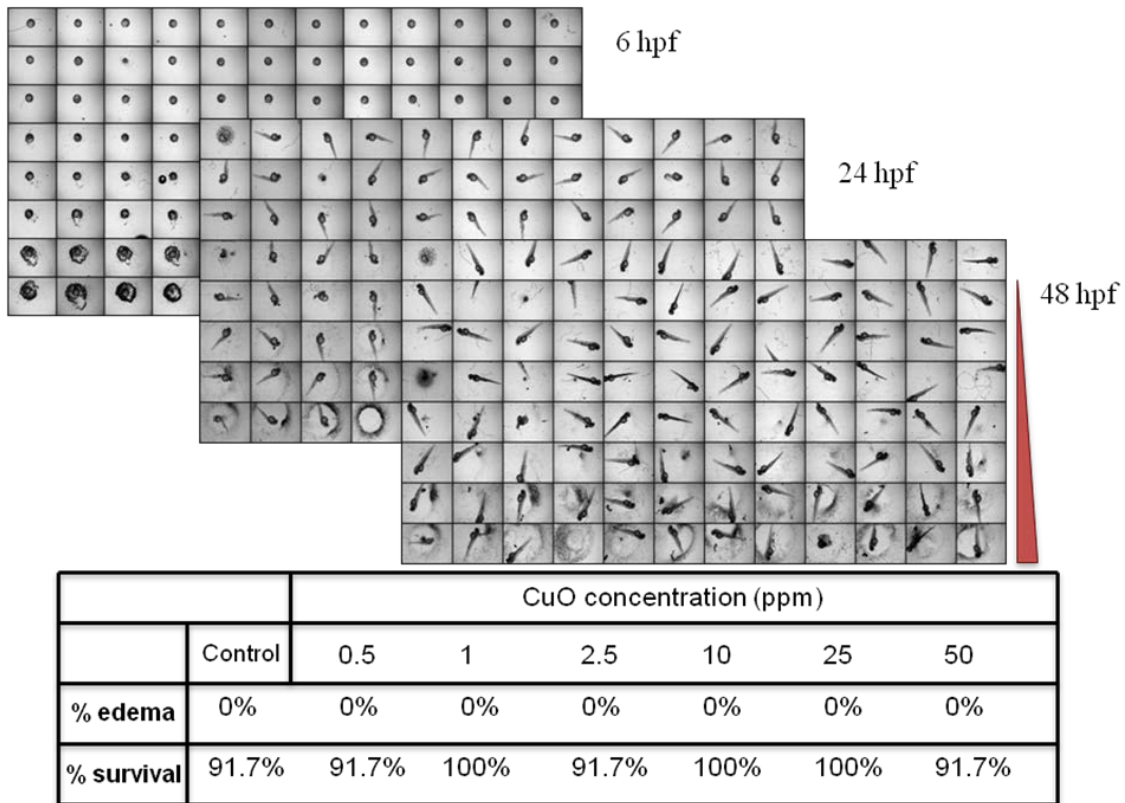


Figure S3. Bright-field automated imaging on dechorionated embryos exposed to CuO nanoparticles. Wild type embryos were harvested at 2 hpf and washed thoroughly using Holtfreter’s medium. Pronase solution (1 mg/mL) was used to enzymatically digest the chorion. Holtfreter’s medium was added immediately to stop the digestion process once the first chorion was dissociated. A single dechorionated embryo was hand-plated in each well of a 96-well plate and exposed to CuO nanoparticles at 4 hpf. Bright-field automated imaging was conducted at 6, 24 and 48 hpf and the rates of edema and survival was scored.

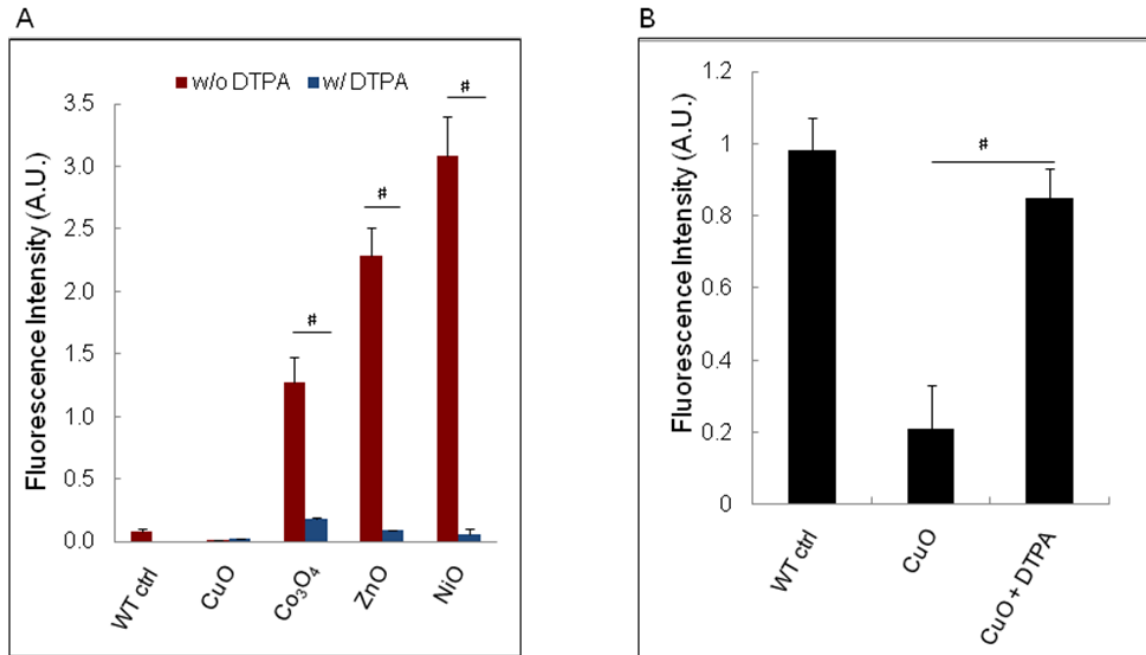


Figure S4. Assessment of fluorescence intensity in embryos injected with metal-sensitive dyes. (A) Fluorescence intensity analysis of embryos microinjected with Newport Green DCF-K (50 μ M). There was a significant difference in the increase in fluorescence intensity of embryos exposed to Co₃O₄, ZnO and NiO compared to wild type controls, suggesting the presence of Co, Zn and Ni ions in the chorion. DTPA (50 μ M) co-exposure resulted in minimum increase of the fluorescence signal through chelation of free metal ions. Because Newport Green DCF-K is insensitive to Cu ions, embryos exposed to CuO nanoparticles did not show a significant increase in fluorescence. (B) Analysis of fluorescent intensity in embryos injected with Phen Green SK (50 μ M). The decrease of fluorescence intensity in embryos exposed to CuO was significantly different from the wild type controls, indicating the presence of free/unbound copper ions. DTPA co-exposure resulted in fluorescence recovery, indicating the chelation of free copper ions by DTPA. Embryos exposed to the dispersed nanoparticles were washed after 24 hours in Holtfreter's medium and injected with 2 nL

of Newport Green DCF-K or Phen Green SK (50 μ M). Fluorescence images of embryos were captured using a Zeiss Observer D1 microscope with exact optical settings (excitation, emission and detection gain level) to obtain quantitative fluorescence intensities. The results were statistically significant at $p < 0.05$ according to student's t-test.

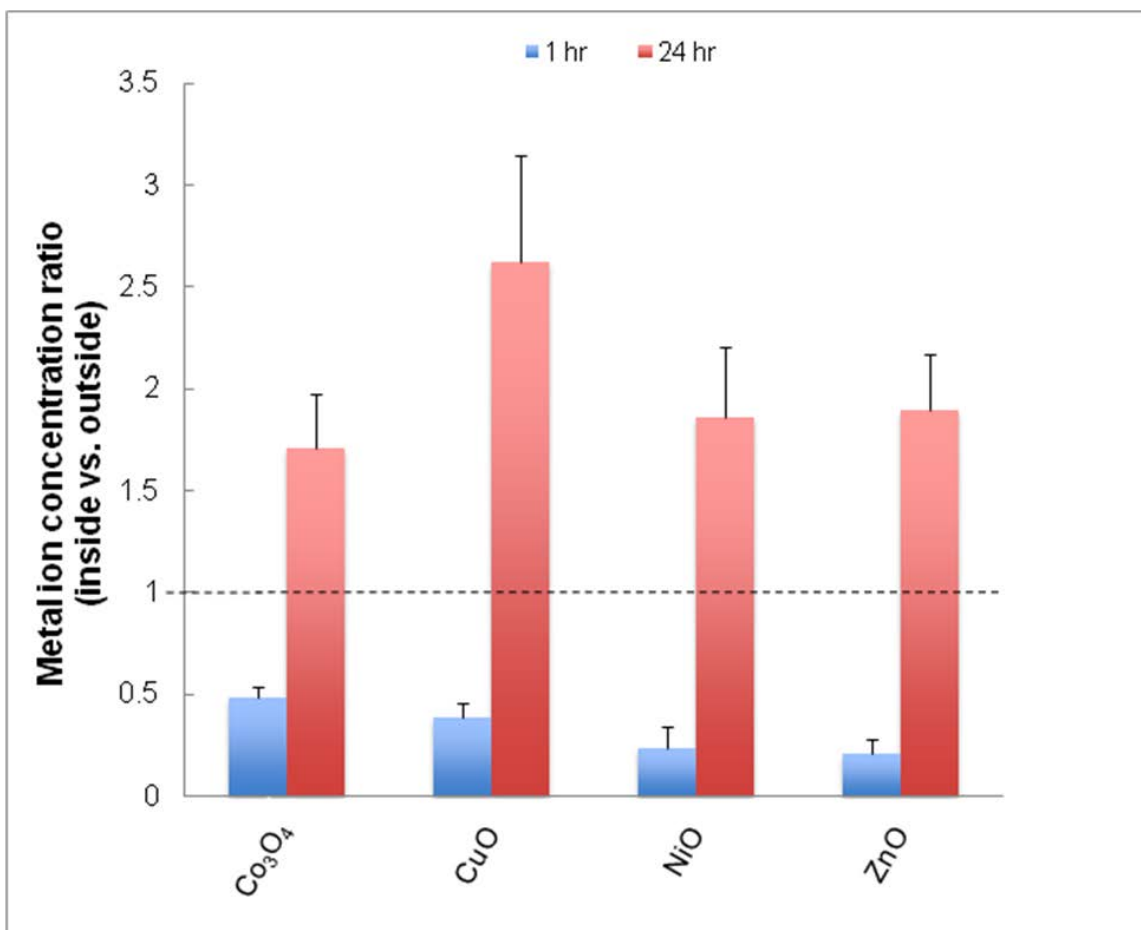


Figure S5. Quantification of metal content inside and outside of chorion by ICP-MS.

The metal content in- and outside the chorion was quantified by ICP-MS analysis and expressed as an inside/outside ratio. Bioconcentration in the chorion could be observed by the increase in the ratio to >1 by 24 hrs. Embryos exposed to nanoparticle dispersions for 1 and 24 hours were washed in Holtfreter's medium, dried, and the chorionic fluid collected after manual breakage of the chorion. The exposure medium was collected for quantification of metal content outside of the chorion.

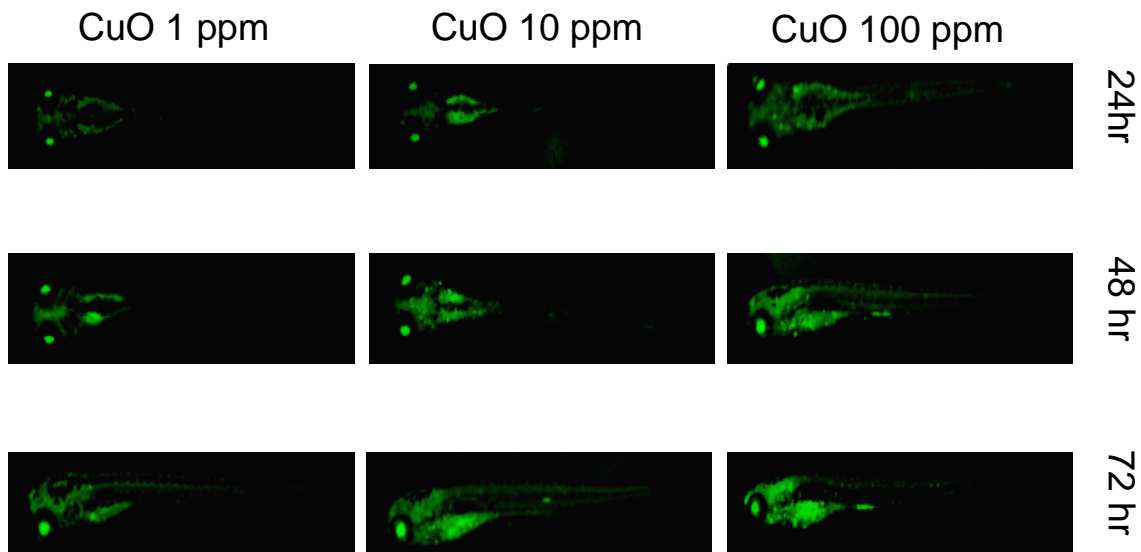


Figure S6. Fluorescence based automated imaging on *hsp70:eGFP* transgenic larvae exposed to CuO nanoparticles. Representative images of transgenic larvae exposed to CuO nanoparticles at increasing concentrations (1, 10 and 100 ppm) and increasing exposure time points (24, 48 and 72 hours). The transgenic larvae were pre-screened to select GFP-positive organisms that were exposed to CuO nanoparticles at 80 hpf. The fluorescence images were captured automatically every 24 hours for 3 consecutive days.

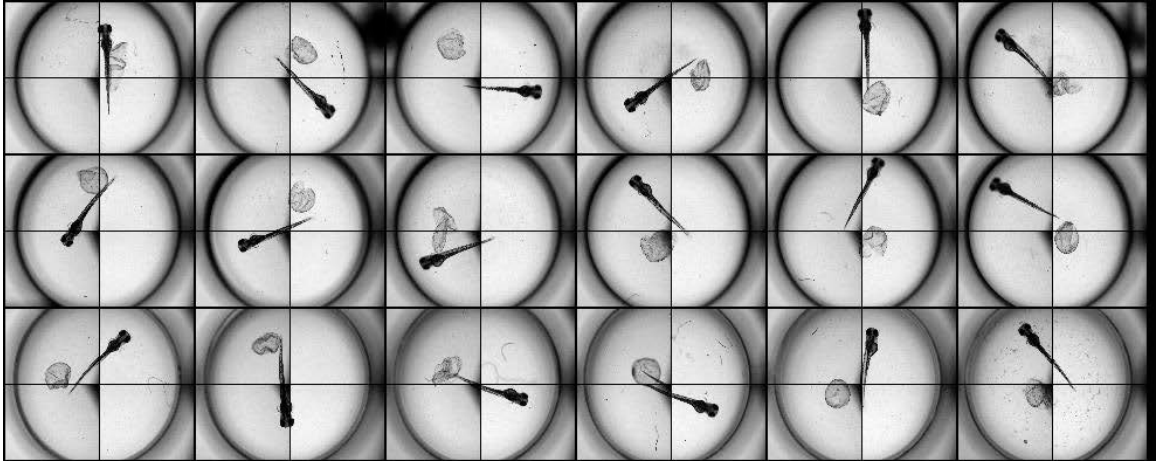


Figure S7. Four quadrant images taken by a bright-field automated microscope to obtain coverage of the entire well in the plate. A recombinant image covering the entire plate surface was attained by merging the four quadrants into a single image that covers the entire well surface. Wild-type embryos were hand picked and placed into each well of a 96-well plate. Co_3O_4 dispersion at 50 ppm was added into each well to start the exposure at 4 hpf. Embryos were kept in an incubator at 28.5 °C and the four quadrant images were merged at 72 hpf to view the hatched larvae. The position of each quadrant image was automatically calculated by defining the type of multwell plates and the center of each well.